Oligodeoxynucleotide Duplexes Containing (5′*S*)-5′-*C*-Alkyl-Modified 2′-Deoxynucleosides: Can an Alkyl Zipper across the DNA Minor-Groove Enhance Duplex Stability?

by **Huldreich Trafelet**[1]), **Serge P. Parel**[2]), and **Christian J. Leumann***

Department of Chemistry and Biochemistry, University of Bern, Freiestrasse 3, CH-3012 Bern
(Phone: (031) 631 4355; fax: (031) 631 3422; e-mail: leumann@ioc.unibe.ch)

Dedicato a *Duilio Arigoni* per il suo 75° compleanno

A series of oligonucleotides containing (5′*S*)-5′-*C*-butyl- and (5′*S*)-5′-*C*-isopentyl-substituted 2′-deoxyribonucleosides were designed, prepared, and characterized with the intention to explore alkyl-zipper formation between opposing alkyl chains across the minor groove of oligonucleotide duplexes as a means to modulate DNA-duplex stability. From four possible arrangements of the alkyl groups that differ in the density of packing of the alkyl chains across the minor groove, three (duplex types **I**–**III**, *Fig. 2*) could experimentally be realized and their duplex-forming properties analyzed by UV-melting curves, CD spectroscopy, and isothermal titration calorimetry (ITC), as well as by molecular modeling. The results show that all arrangements of alkyl residues within the minor groove of DNA are thermally destabilizing by 1.5–3°/modification in T_m. We found that, within the proposed duplexes with more loosely packed alkyl groups (type-**III** duplexes), accommodation of alkyl residues without extended distorsion of the helical parameters of B-DNA is possible but does not lead to higher thermodynamic stability. The more densely packed and more unevenly distributed arrangement (type-**II** duplexes) seems to suffer from ecliptic positioning of opposite alkyl groups, which might account for a systematic negative contribution to stability due to steric interactions. The decreased stability in the type-**III** duplexes described here may be due either to missing hydrophobic interactions of the alkyl groups (not bulky enough to make close contacts), or to an overcompensation of favorable alkyl-zipper formation presumably by loss of structured H_2O in the minor groove.

1. Introduction. – The stability of the DNA double helix is controlled by a subtle balance of attractive and repulsive forces. The attractive forces are mainly H-bonding and stacking interactions between the bases as well as desolvation effects upon base-pair formation. Repulsive forces include the entropic penalty upon conformational organization of single strands for duplex formation as well as electrostatic repulsion due to the negative charges of the phosphodiester backbone. The effect of conformational preorganization of DNA single strands on duplex formation as well as electrostatic effects have been addressed in the past by the study of oligonucleotide analogues displaying conformationally more-flexible or more-constrained sugar-phosphate backbones [1–3], or by oligonucleotide analogues with noncharged backbone structures.

Assessing the contribution of solvation on the stability of the double helix, however, is more difficult. It is known from ultrasound experiments combined with density

---

[1]) Present address: *Siegfried AG*, CH-4800 Zofingen.

[2]) Present address: *Discovery Partners Int.*, Gewerbestr. 16, CH-4123 Allschwil.

measurements that solvation is largely sequence and base-pair dependent [4]. *Raman*-spectroscopy investigations are in agreement with *ca.* 30 molecules of H_2O for the first hydration sphere of a nucleotide pair in a B-DNA duplex together with *ca.* 5–6 that are not exchangeable [5]. It is thought that the H_2O molecules are arranged in chains bridging opposite phosphodiester groups [6]. Theory predicts that H_2O bridging of polar atoms is significantly perturbing ligand–receptor binding in biomacromolecules [7]. Thus, it is likely that structured H_2O, as in the first hydration sphere of DNA, significantly influences duplex stability. Structured H_2O in DNA duplexes is in part visible by X-ray crystallography. Especially, a recent, detailed analysis of the *Dickerson-Drew* dodecamer duplex at below 1.0-Å resolution revealed well-ordered H_2O molecules as, *e.g.*, in the spine of hydration along the AATT sequence tract [8].

To investigate solvation and hydrophobic effects in more detail, we set out to study 5′-alkyl-substituted oligonucleotide analogues containing butyl or isopentyl side chains at the position of $H_{pro\text{-}S}$–C(5′) (*Fig. 1*). A closer inspection of a B-DNA helix reveals that $H_{pro\text{-}S}$–C(5′) points into the minor groove almost parallel to the helical axis. Thus,

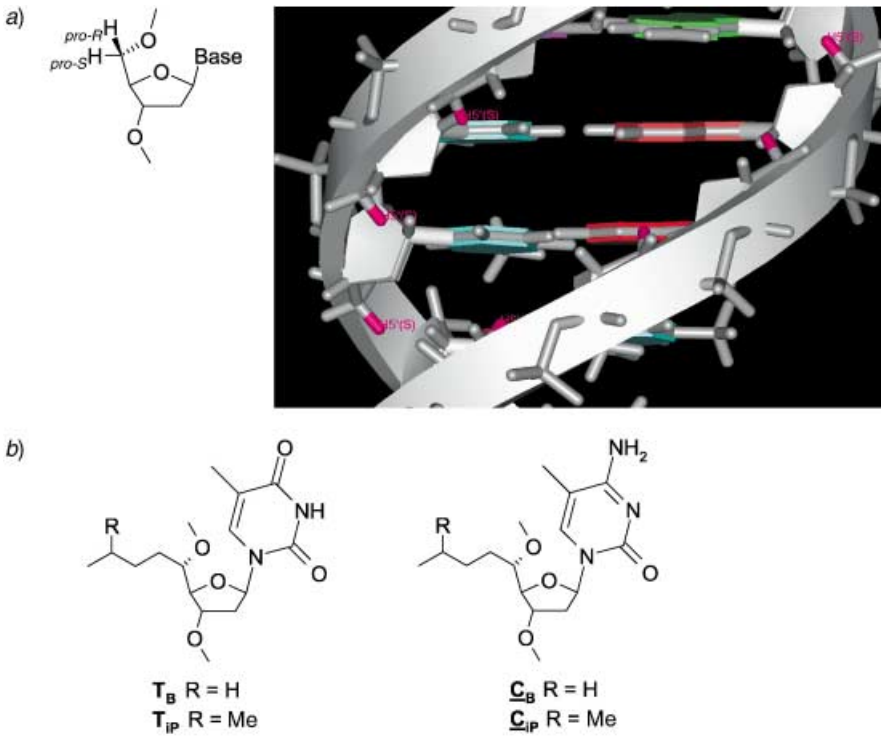

Fig. 1. a) *Relative location of the* $H_{pro\text{-}S}$–*C(5′)* (represented by H5′(S) in pink) *in a B-DNA double helix* (the $H_{pro\text{-}S}$–C(5′) roughly point along the helical axis across the minor groove and the $H_{pro\text{-}R}$–C(5′) point away from the helical axis towards the solvent). b) *Representation of the (5′*S*)-5′-*C*-butyl- and (5′*S*)-5′-*C*-isopentyl nucleosides* T_B *and* T_{ip} *as well as* C_B *and* C_{ip} *of the bases thymine and 5-methylcytosine, respectively used in this study.*

its substitution by an alkyl chain brings the latter into direct competition with solvate H_2O. Given the width of the minor groove of *ca.* 7 Å, a chain length of four C-atoms, branched and nonbranched, seemed appropriate. A further challenging question behind this study was whether alkyl chains arranged on opposite sides of the minor groove would form a hydrophobic zipper, in much the same way as the leucine-zipper motif [9] occurring in proteins does (see below, *Fig. 2*), and whether this could be a general, base-sequence-independent approach to modulate DNA-duplex stability. In the past, 5′-alkylated oligonucleotides carrying a variety of different functionalized and nonfunctionalized alkyl groups were already investigated in the context of antisense research [10–12]. It was shown that single and multiple substitutions at random positions of an oligonucleotide lead to a significant reduction in thermal stability of corresponding duplexes with complementary DNA or RNA.

We already reported the preparation of the requisite nucleosides and the corresponding building blocks for DNA synthesis, depicted in *Fig. 1* [13]. Here we disclose the synthesis of the (5′*S*)-5′-*C*-butyl- and (5′*S*)-5′-*C*-isopentyl-substituted oligonucleotides together with an analysis of the thermodynamics of duplex formation by UV-melting-curve analysis and isothermal titration calorimetry (ITC) as well as a structural analysis by CD spectroscopy and molecular modelling.

2. Results and Discussion. – 2.1 *Sequence Design.* Given the right-handed-helical nature of DNA, careful sequence design of oligonucleotides was necessary. In principle, four different arrangements of alkyl chains are possible in the minor groove, termed types **I**–**IV**, that are schematically represented in *Fig. 2*. There are two possible motifs with alkylated residues in adjacent positions (type **I** and **II**) and two motifs with the alkylated nucleosides in alternating positions (type **III** and **IV**). Arrangement of the alkylated residues at the 5′-end results in a geometry where the alkyl chains point into different segments of the minor groove (type **I**). In this arrangement, alkyl-zipper formation is impossible. Introducing the alkylated nucleosides towards the 3′-end as in type **II** leads to an arrangement in which the alkyl chains lie in the same segment of the minor groove. Given that consecutive residues are alkylated, this corresponds to the 'closest-packing motif' in a putative zipper, where contacts between the alkyl chain of nucleoside *n* can occur with those of nucleosides $n+3$ and $n+4$ of the opposite strand. Substituting only every second nucleoside with alkyl groups results in less-dense packing (types **III** and **IV**). There is a structural difference between contacts of alkyl chains of residues *n*, $n+3$ (type **III**) and *n*, $n+4$ (type **IV**), the former leading to a more-uneven distribution of alkyl chains in the minor groove compared to the latter. With only the alkylated pyrimidine nucleosides at hand, we were able to experimentally investigate duplexes of type **I**–**III**. Investigation of duplexes of type **IV** would have required the use of alkylated purine nucleosides. The corresponding synthesized oligonucleotides and their sequence information is given in *Table 1*.

2.2. *Synthesis.* The syntheses of oligonucleotides were performed on a commercial DNA synthesizer by using standard phosphoramidite chemistry. The coupling times for the alkylated nucleoside building blocks was extended to 8–10 min. That of natural building blocks immediately following a modified unit was set to 5 min. Coupling yields between modified units were in the range of 93–98%, as determined by the pixyl assay. Detachment from the solid support and deprotection followed again standard

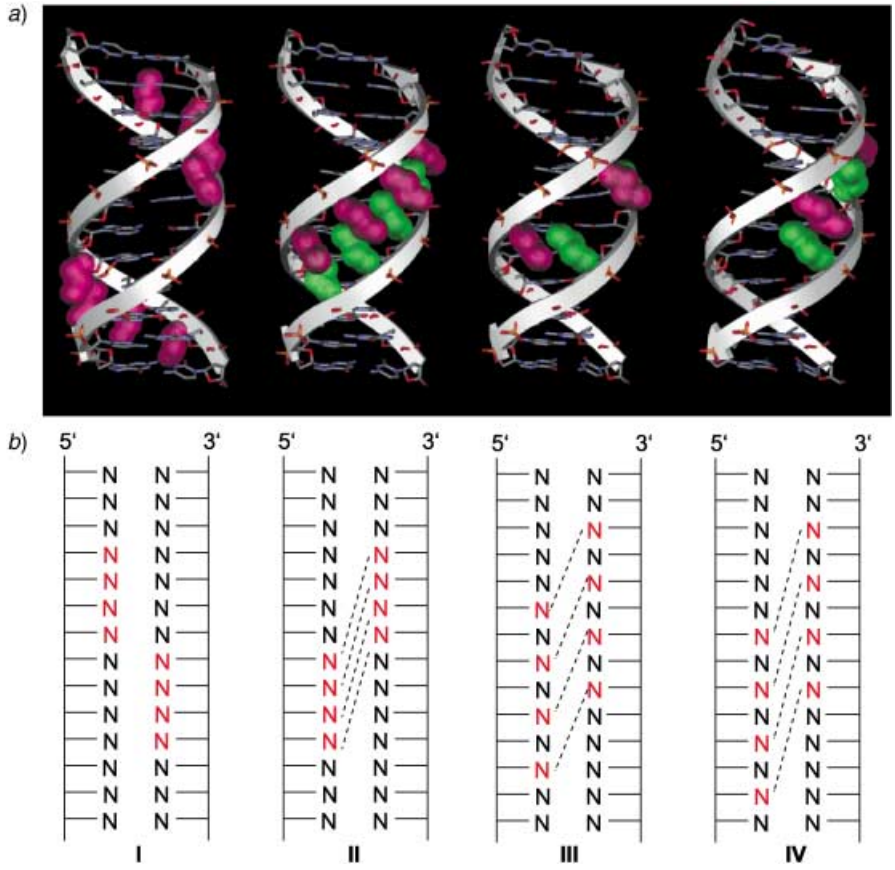

Fig. 2. a) *Molecular models of the sequence-dependent arrangements of the alkyl groups of (5′*S*)-5′-alkylnucleosides in the minor groove of DNA and* b) *schematic representation of corresponding DNA-duplex types* **I**–**IV** *with alkylated nucleosides drawn in red* (dashed lines indicate adjacent alkyl groups). In the sequence motif **I**, the alkyl groups of both strands extend in different segments of the minor groove. In the three remaining motifs, the alkyl groups point into the same segment of the minor groove allowing for the formation of an alkyl zipper. The sequence **II** thereby corresponds to a 'closest-packing' model with adjacent alkylated nucleosides, while the two motifs **III** and **IV** correspond to the two possible arrangements in alternately (*n vs. n* + 3 and *n vs. n* + 4) substituted alkyl-DNA. Due to the fact that only (5′*S*)-5′-alkyl-substituted pyrimidine (and not purine) nucleosides were at our disposal, the motif **IV** could not be investigated experimentally.

procedures (conc. NH_3 solution, 55°, 16 h). Crude oligonucleotides were purified by anion-exchange HPLC and their purity controlled by reversed-phase HPLC. We noted significantly higher retention times for the alkylated oligonucleotides, even in ion-exchange HPLC. All modified oligonucleotides were characterized by MALDI-TOF mass spectrometry. The molecular masses were found to be within 1‰ of the expected mass in all cases (see *Exper. Part*).

2.3. *Selfcomplementary Sequences.* In first experiments, we investigated duplex-formation properties of the selfcomplementary oligonucleotides of the series **1**–**3**

Table 1. *Base-Sequence Information of Oligonucleotides Investigated*

	Selfcomplementary	Type		Non-selfcomplementary	Type
1.0	d(GCGCTTTTAAAAGCGC)	–	**5.0S**	d(TAC̲AGGAC̲CTC̲AGT)	–
1.4	d(GCGC$T_BT_BT_BT_B$AAAAGCGC)	I	**5.0A**	d(AC̲TGAGGTC̲CTGTA)	
2.0	d(GCGCAAAATTTTGCGC)	–	**5.1S**	d(TAC̲AGGAC$_B$C̲$_B$C̲$_B$T$_B$C̲$_B$AGT)	II
2.4	d(GCGCAAAA$T_BT_BT_BT_B$GCGC)	II	**5.1A**	d(AC̲TGAGGT$_B$C̲$_B$C̲$_B$T$_B$GTA)	
3.0	d(GATATATATATATC)	–	**5.2S**	d(TAC̲AGGAC$_{iP}$C̲$_{iP}$T$_{iP}$C̲$_{iP}$AGT)	II
3.1	d(GATAT$_B$AT$_B$AT$_B$AT$_B$AT$_B$C)	III	**5.2A**	d(AC̲TGAGGT$_{iP}$C̲$_{iP}$C̲$_{iP}$T$_{iP}$GTA)	
			6.0S	d(GC̲ATAC̲GTAC̲ACC̲G)	–
			6.0A	d(C̲GGTGTAC̲GTATGC)	
			6.1S	d(GC̲ATAC$_B$GT$_B$AC$_B$AC̲$_B$C̲G)	III
			6.1A	d(C̲GGTGT$_B$AC̲$_B$GT$_B$AT$_B$GC)	
			6.2S	d(GC̲ATAC̲$_{iP}$GT$_{iP}$AC̲$_{iP}$AC̲$_{iP}$C̲G)	III
			6.2A	d(C̲GGTGT$_{iP}$AC̲$_{iP}$GT$_{iP}$AT$_{iP}$GC)	

containing butyl chains (*Table 1*, left columns), *i.e.* **1.0** *vs.* **1.4**, **2.0** *vs.* **2.4**, and **3.0** *vs.* 3.1, by UV-melting-curve analysis. Selfcomplementarity was chosen primarily as a means to economize on the number of oligonucleotides that had to be synthesized. The T_m data at neutral pH and at three different NaCl concentrations are summarized in *Table 2*. Representative melting curves are depicted in *Fig. 3*.

Table 2. T_m [°] *Data of Selfcomplementary (5′S)-5′-Alkyloligonucleotides at Three Different NaCl Concentrations.* Duplex conc. = 1.5 μM in 10 mM NaH_2PO_4, pH 7.0.

	Type	T_m^1 [a])	ΔT_m^1	T_m^1 [a])	ΔT_m^1	T_m^1 [a])	ΔT_m^1	T_m^2 [b])		
		0 mM		150 mM		1 M		0 mM	150 mM	1 M
1.0	–	39.4	–	53.1	0	55.9	–	64.9	72.7	75.8
1.4	**I**	21.9	– 2.2	29.2	– 3.0	32.8	– 2.9	56.4	61.6	65.0
2.0	–	44.4	–	52.3	0	65.0[c])	–	63.3	68.2	72.7
2.4	**II**	24.2	– 2.5	33.5	– 2.4	36.7	– 3.5	63.3	72.8	76.8
3.0	–	30.2	–	33.4	0	40.5	–	n.d.[d])	n.d.[d])	n.d.[d])
3.1	**III**	14.9	– 1.5	21.0	– 1.2	20.9	– 2.0	n.d.[d])	n.d.[d])	n.d.[d])

[a]) T_m at lower temperature corresponding to a bimolecular-duplex → hairpin transition. [b]) T_m at higher temperature corresponding to monomolecular hairpin melting. [c]) Only one transition observable. [d]) n.d. = Not determined.

It becomes clear that with the exception of the duplexes of the series **3**, *i.e.*, **3.0** and **3.1**, biphasic transitions occur irrespective whether modified residues are involved or not. The first transition in the melting curves (T_m^1) corresponds to a bimolecular-duplex → monomolecular-hairpin transition, while the second (T_m^2) reflects melting of the hairpin structures to random-coiled single strands. Hairpin formation occurs not unexpectedly and is a consequence of the chosen sequence, with multiple GC repeats at the ends, which are known to form stable hairpin stems. In the context of a putative butyl-zipper motif, the first (bimolecular) transition is certainly more meaningful, as the alkylated nucleosides are at least in part located in the loop region in the hairpin structures, and, thus, in a nonregular structural alignment. Inspection of the T_m data

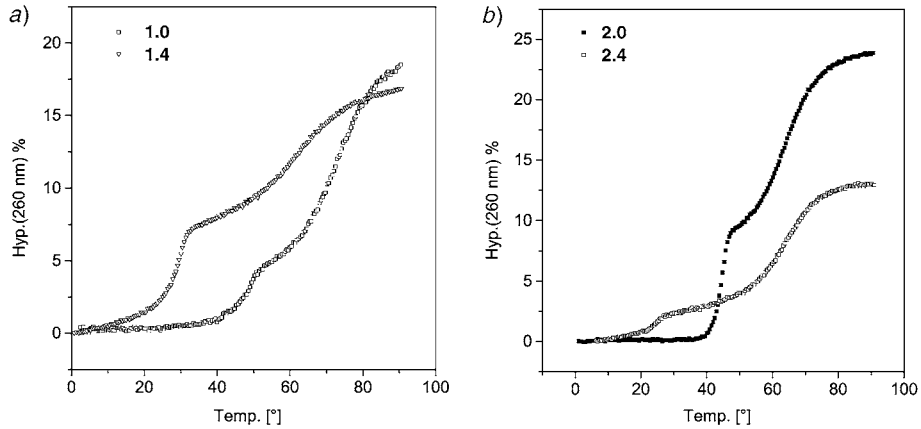

Fig. 3. *UV Melting curves* (260 nm) *of the selfcomplementary duplexes showing a bimolecular duplex → hairpin transition at lower temperature and hairpin melting at higher temperature:* a) *duplexes* **1.0** *and* **1.4** (1.6 μM in 10 mM NaH_2PO_4, 150 mM NaCl, pH 7.0) *and* b) *duplexes* **2.0** *and* **2.4** (1.6 μM in 10 mM NaH_2PO_4, pH 7.0).

reveals that, irrespective of the ionic strength of the solvent, in the duplex **1.4** of type **I**, the butyl groups lead to a destabilization of the duplex by ΔT_m −2.2 to −3.0°/modification. In the case of the duplex **2.4** of type **II**, destabilization is similar, with a ΔT_m of − 2.4 to −3.5°/modification. The duplex **3.1** of type **III** shows less-pronounced destabilization, with a ΔT_m of − 1.2 to −2.0°/modification. The melting of the hairpin structures (T_m^2) vary much less as a function of the type of alkyl modification and are an indication that their effect on the stability of a loop structure is less pronounced.

A structural investigation of the duplexes **1.4**, **2.4**, and **3.1** by CD spectroscopy reveals the largest differences between alkylated and nonalkylated duplexes to occur in series 2 (*Fig. 4,b*) displaying the tightest packing of butyl chains (type **II**). Here the CD trace of **2.4** is positively shifted over the whole wavelength range. The reason for this behavior is unknown. The CD traces of **1.4** and **3.1** are similar to those of the unmodified duplexes and differ only in slight reductions of the maximum and minimum ellipticities.

Thus the study of the selfcomplementary sequences revealed a significant dependence of stability and conformation as a function of the position of the butyl chains in the sequence. It appears that the structural motif **II** with the highest density of alkyl groups in opposite positions of the minor groove leads to the strongest duplex destabilization observed, associated with a change in duplex conformation. Duplex motif **III** is the least destabilizing. The results so far are consistent with the view that the positive energetic contributions of hydrophobic interactions upon zipper formation of butyl chains is overwhelmed by negative contributions of desolvation of ordered H_2O. Alternatively, we can not exclude that conformational strain in the phosphodiester backbone, imposed by the butyl side chains, is responsible for the loss in duplex stability. We note that there is no rigorous proof for an alkyl-zipper arrangement.

2.4. *Non-Selfcomplementary Sequences.* To circumvent duplex → hairpin equilibria, which render an exact determination of thermodynamic data of duplex formation difficult, and to perform ITC experiments, we switched to non-selfcomplementary

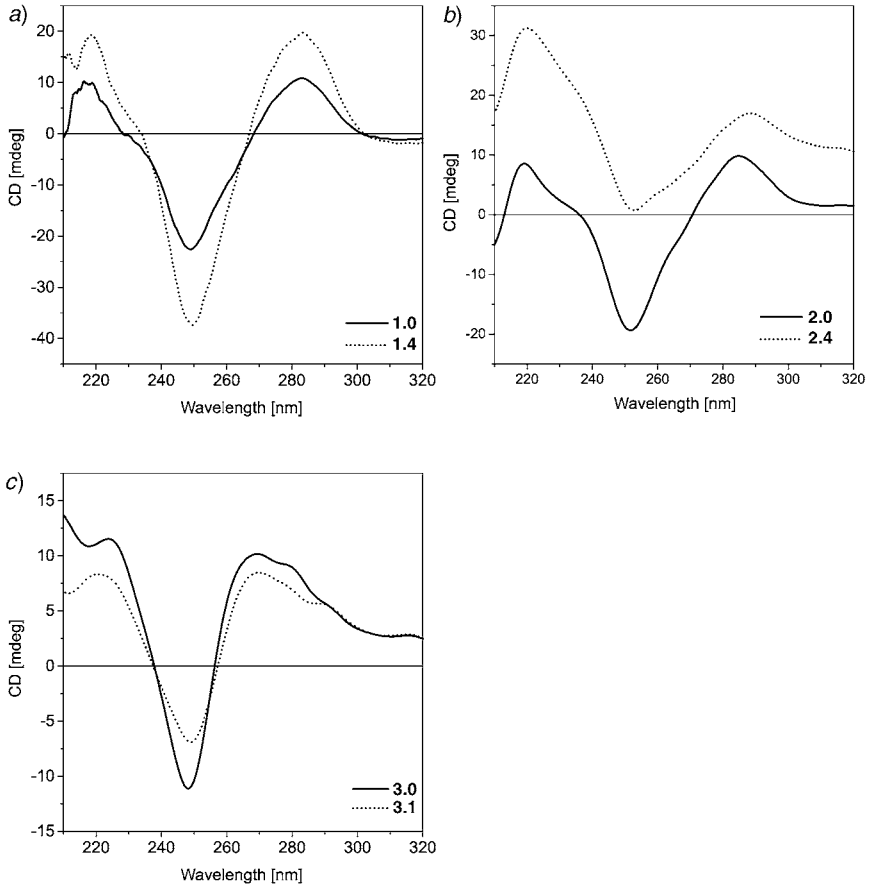

Fig. 4. *CD Spectra at 10° of the selfcomplementary duplexes at 150 mM NaCl:* a) **1.0** *and* **1.4**, b) **2.0** *and* **2.4**, *and* c) **3.0** *and* **3.1**. Conditions as described in *Table 2*.

oligodeoxynucleotides that exhibit butyl- and isopentyl-group distribution patterns as in type **II** and **III** (*Table 1*, right columns, series **5** and **6**). Again we first measured UV melting curves. The corresponding T_m data for the relevant duplexes at three different NaCl concentrations are summarized in *Table 3*. Corresponding melting curves are depicted in *Fig. 5*.

Not unexpectedly, we observed similar behavior as in the case of the selfcomplementary oligonucleotides. Destabilization is strongest in the case of the type-**II** duplexes with a ΔT_m of $-2.6°$/butyl modification and is largely similar irrespective of the ionic strength of the medium. Destabilization is slightly stronger in the case of the isopentyl modification. Duplexes of type **III** show moderate destabilization in the range of ΔT_m $-2.1°$/butyl modification. Also in this sequence context the isopentyl modification is generally more destabilizing by $\Delta\Delta T_m$ $-0.3°$/butyl modification.

The corresponding CD spectra (*Fig. 6*) indicate relatively similar structure and conformations for duplexes of type **II** and **III** (series **5** and **6**) with one notable

Table 3. T_m [°] *Data of Non-selfcomplementary (5′S)-5′-Alkyloligonucleotides at Three Different NaCl Concentrations.* Duplex conc. = 1.5 μM in 10 mM NaH_2PO_4, pH 7.0.

	Type	T_m	ΔT_m	T_m	ΔT_m	T_m	ΔT_m
		0 mM		150 mM		1 M	
5.0S · 5.0A	–	51.0	–	64.7	–	69.7	–
5.1S · 5.1A	**II**	30.3	– 2.6	43.5	– 2.7	47.9	– 2.7
5.2S · 5.2A	**II**	28.0	– 2.9	42.3	– 2.8	49.0	– 2.6
6.0S · 6.0A	–	48.9	–	62.3	–	66.6	–
6.1S · 6.1A	**III**	32.4	– 2.1	45.7	– 2.1	49.1	– 2.2
6.2S · 6.2A	**III**	30.0	– 2.4	43.0	– 2.4	47.7	– 2.4

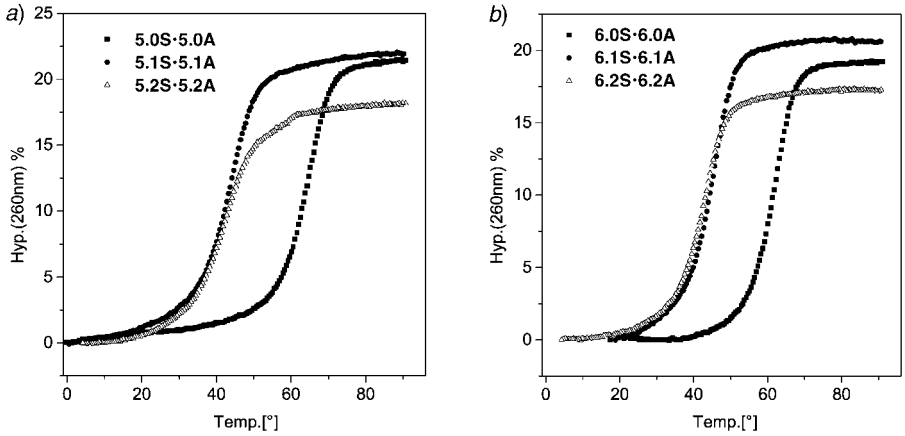

Fig. 5. *UV Melting curves* (260 nm) *of the non-selfcomplementary duplexes of the series* **5** *and* **6**. Exper. conditions as indicated in *Table 3* (150 mM NaCl).

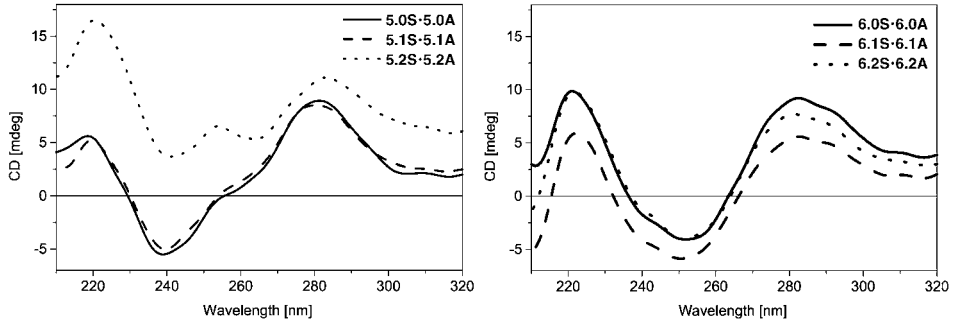

Fig. 6. *CD Spectra at 10° of non-selfcomplementary duplexes of the series* **5** *and* **6**. Conditions as indicated in *Table 3* (150 mM NaCl).

exception. The duplex **5.2S · 5.2A** containing isopentyl side chains shows significantly shifted ellipticities towards the positive range and behaves, thus, similarly as the selfcomplementary duplex **2.4**. This does not occur with the duplex **5.1S · 5.1A** displaying only butyl groups in the identical sequence context.

To investigate the effect of a change in solvent, we measured T_m data in buffered 50% ^{i}PrOH/H_2O (*Table 4*). Alkyl-group-containing oligonucleotides uniformly show much stronger destabilization of the double helix relative to buffered H_2O than unmodified oligonucleotides. Differences in T_m relative to buffered H_2O can be as high as $-30°$ for modified duplexes relative to $-8°$ for natural duplexes. This dramatic loss of stability can be an indication of weakening of the hydrophobic interaction of an alkyl zipper with increasing amounts of organic solvent.

Table 4. T_m [°] *Data of Non-selfcomplementary (5′*S*)-5′-Alkyloligonucleotides in ^{i}PrOH/H_2O 50 : 50.* Duplex conc. = 1.5 μM in 10 mM NaH_2PO_4, pH 7.0 (no NaCl).

	Type	T_m		ΔT_m
		50% ^{i}PrOH/H_2O	H_2O	
5.0S · 5.0A	–	43.0	51.0	– 8.0
5.1S · 5.1A	**II**	*ca.* 0	30.3	*ca.* – 30.3
6.0S · 6.0A	–	40.9	48.9	– 8.0
6.1S · 6.1A	**III**	*ca.* 0	32.4	*ca.* – 32.4

The results in the series of the non-selfcomplementary sequences are so far consistent with the observations made for the selfcomplementary sequences. The strong sensitivity of duplex formation towards organic solvents in the alkyloligonucleotide series clearly highlights the importance of the effect of differential solvation on duplex stability.

To factorize the observed thermodynamic stabilities into enthalpic and entropic contributions, we measured thermodynamic data of duplex formation by two different methods, namely by indirect (model-dependent) curve-fitting procedures to the experimental melting-curve, and by direct (model-independent) isothermal titration calorimetry (ITC). The *van't Hoff* enthalpies as obtained from the UV melting curves consistently show a decrease of the pairing enthalpy term ΔH^{vH} in duplexes containing alkyl residues (*Table 5*). ΔH^{vH} is reduced by *ca.* 3.4 kcal/mol per modification in the case of butyl residues, and by *ca.* 5 kcal/mol per modification in the case of isopentyl residues, irrespective of the structural motif (type **II** or **III**). The loss in pairing enthalpy is partly compensated by the entropy term, as often observed in oligonucleotide association.

Table 5. Van't Hoff *Thermodynamic Data for Duplex Transitions from UV Melting Curves* ($1/T_m$ *vs.* ln(c) plots)

	Type	ΔH^{vH} [kcal/mol]	ΔS^{vH} [cal/K · mol]	ΔG^{vH} [kcal/mol][a])
5.0S · 5.0A	–	– 96.1 ± 0.02	– 257.3 ± 0.06	– 18.2
5.1S · 5.1A	**II**	– 70.6 ± 0.05	– 195.2 ± 0.1	– 11.5
5.2S · 5.2A	**II**	– 56.3 ± 0.06	– 150.7 ± 0.2	– 10.6
6.0S · 6.0A	–	– 107.9 ± 0.04	– 294.8 ± 0.1	– 18.6
6.1S · 6.1A	**III**	– 89.8 ± 0.06	– 254.0 ± 0.2	– 12.8
6.2S · 6.2A	**III**	– 71.1 ± 0.05	– 198.0 ± 0.2	– 11.1

[a]) Calc. for T 303 K.

A different source of thermodynamic data is ITC. With this method, which we had used successfully before in the context of measuring thermodynamic data of DNA duplex and triplex formation [14], not only ΔH but also association constants can be measured in the same experiment at a predetermined temperature. We performed ITC on the duplexes of the series **5** and **6** at 30°. A typical ITC trace is reproduced in *Fig. 7*, the corresponding data are summarized in *Table 6*.

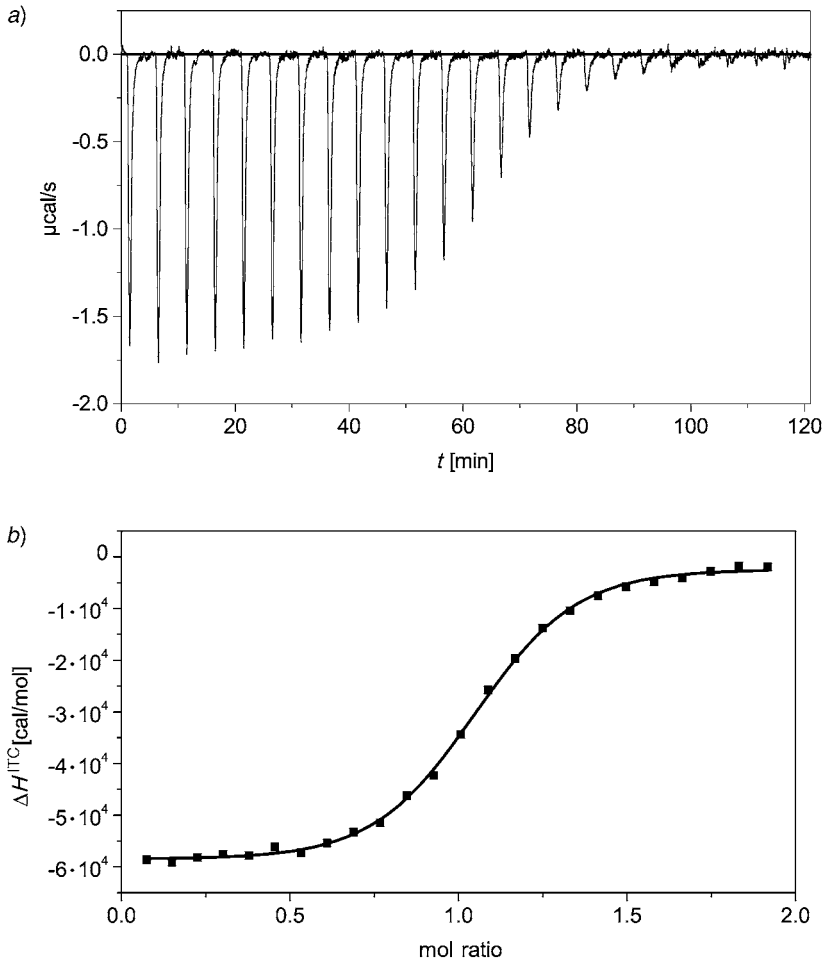

Fig. 7. *Data from isothermal titration calorimetry* (ITC) *of* **5.2A** (11.1 µM), *titrated with* **5.2S** (132.2 µM) *in 10 mM* NaH_2PO_4 and *150 mM NaCl, pH 7.0:* a) *untreated heat signal* (Δcp) vs. *time*; b) *sigmoidal fit of the integrated and normalized heat signal* (ΔH^{ITC}) *as a function of the molar ratio of titrants*

For the duplexes of series **5**, the association constants drop by approximately 100-fold after introducing the 5′-alkylnucleosides into the oligonucleotides. The diminished association constants translate into a difference in ΔG^{ITC} of *ca.* 3 kcal/mol. There seems

Table 6. *Thermodynamic Data from Isothermal Titration Calorimetry* (ITC) *for the Non-selfcomplementary Duplexes at 30.5 ± 0.5° in 10 mM NaH_2PO_4 and 150 mM NaCl, pH 7.0*

	Type	K_{ass}	ΔH^{ITC} [kcal/mol]	ΔS^{ITC} [cal/K · mol]	ΔG^{ITC} [kcal/mol][a])
5.0S · 5.0A	–	$(4.98 \pm 1.96) \cdot 10^8$	-81.6 ± 0.3	-228.7 ± 4.4	-12.1 ± 0.8
5.1S · 5.1A	**II**	$(4.62 \pm 0.5) \cdot 10^6$	-55.0 ± 1.4	-150.1 ± 4.8	-9.3 ± 1.5
5.2S · 5.2A	**II**	$(4.38 \pm 0.3) \cdot 10^6$	-59.5 ± 1.3	-165.9 ± 4.4	-9.2 ± 1.3
6.0S · 6.0A	–	$(4.92 \pm 2.13) \cdot 10^8$	-83.9 ± 1.1	-236.3 ± 4.3	-12.2 ± 1.3
6.1S · 6.1A	**III**	$(2.25 \pm 0.4) \cdot 10^6$	-48.9 ± 1.6	-131.8 ± 5.6	-8.8 ± 1.7
6.2S · 6.2A	**III**	$(6.09 \pm 0.6) \cdot 10^6$	-77.9 ± 1.1	-225.9 ± 3.8	-9.4 ± 1.2

[a]) Calc. for 303 K.

to be no major difference in K_{ass} in relation to the nature of the side chain (butyl *vs.* isopentyl). The pairing enthalpy ΔH^{ITC} is sharply reduced relative to that of the unmodifed duplex by *ca.* 3.3 kcal/mol per modification. Thus the trend is similar to that determined by the UV-melting-curve analysis (ΔH^{vH}), but there seems to be no significant difference in ΔH^{ITC} as a function of the nature of the alkyl side chain in the type-**II** system. In type-**III** duplexes of the series **6**, clear differences with respect to the nature of the alkyl chains can be observed. While the association constants of the duplexes **6.1S · 6.1A** and **6.2S · 6.2A** vary only by *ca.* threefold and are again two orders of magnitude smaller than that of the unmodified duplex, there is a marked difference in the enthalpy and entropy terms. In the duplex containing the isopentyl chains, ΔH^{ITC} is only slightly decreased and is still in the range of that of the unmodified duplex, whereas ΔH^{ITC} for the duplex **6.1S · 6.1A** is largely in line with those measured for the series **5**. Thus, duplex **6.2S · 6.2A** is clearly entropically destabilized.

A comparison and interpretation of the extracted *van't Hoff* and ITC enthalpies should take into account the different structural transitions associated with the respective experiment. This becoms clearer by invoking a closed thermodynamic cycle (*Fig. 8*) as discussed in a similar context by *Vesnaver* and *Breslauer* [15].

ΔH^{vH} Data from UV melting curves describe the transition of an ordered double helix at low temperature to random-coiled single strands at high temperature. This corresponds to ΔH_3 in the cycle of *Fig. 8*. On the other hand, ΔH^{ITC} characterizes ordered duplex formation at 30° from single-strand structures at the same temperature and is described by ΔH_2 in the thermodynamic cycle. Thus, the differences of ΔH^{ITC} and ΔH^{vH} reflect the enthalpy change of the single strands at low (ordered) and high (disordered) temperature (ΔH_1 in *Fig. 8*). The calculated $\Delta\Delta H$ values are listed in *Table 7*.

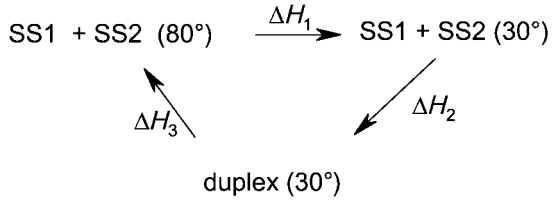

Fig. 8. *Thermodynamic cycle for duplex → single-strand* (SS) *transitions.* Experimentally accessible are ΔH_2 from isothermal titration calorimetry and ΔH_3 from UV-melting-curve analysis.

Table 7. *Comparison of Duplex Dissociation Enthalpies from Isothermal Titration Calorimetry* (ITC) *and* van't Hoff *Enthalpies from UV Melting Curves*

	Type	ΔH^{ITC} [kcal/mol] (ΔH_2)	ΔH^{vH} [kcal/mol] (ΔH_3)	$\Delta\Delta H$ [kcal/mol] (ΔH_1)
5.0S · 5.0A	–	− 81.6	− 96.1	+ 14.5
5.1S · 5.1A	**II**	− 55.0	− 70.6	+ 15.5
5.2S · 5.2A	**II**	− 59.5	− 56.3	− 3.2
6.0S · 6.0A	–	− 83.9	− 107.9	+ 24.0
6.1S · 6.1A	**III**	− 48.9	− 89.8	+ 40.9
6.2S · 6.2A	**III**	− 77.9	− 71.1	− 6.8

Inspection of the data shows that the duplexes containing isopentyl chains differ markedly from the others in that the values for ΔH_1 in the thermodynamic cyle ($\Delta\Delta H$) are slightly negative, whereas they are significantly positive in the case of the other duplexes. An interpretation of this fact points to stabilized (more ordered) single-strand structures at low temperature in the unmodified or butyl-modified oligonucleotides, and nonstabilized (similarly ordered) single-strand structures of the isopentyl-modified oligonucleotides at low and high temperatures. We note that the given interpretation strongly relies on the correctness of the two-state model applied in the determination of the ΔH^{vH} data.

Unfortunately again, in the absence of detailed structural data, it is not possible to attribute the loss of overall thermodynamic stability as a function of the (5′*S*)-5′-alkyl modification to favorable zipper formation associated with unfavorable desolvation of ordered H_2O in the minor groove. Similarly, despite of the available thermodynamic data, we cannot exclude that structural and conformational effects imposed by the introduction of the alkyl residues may also play a role.

2.5. *Modeling.* To get a glimpse at possible structures for (5′*S*)-5′-alkyloligonucleotide representatives of the types **II** and **III**, we first modeled the selfcomplementary oligonucleotide **2.4**. As can be seen from *Fig. 9*, the zipper motif of the opposing butyl side chains in this densely packed type-**II** duplex is far from ideal due to the fact that the point of attachment of the alkyl chains on the opposing sides of the minor groove are eclipsed instead of staggered. As a result, the butyl chains have to arrange themselves to avoid steric clash. This leads to butyl chains that are turned out or that are pushed into the minor groove. This steric clash has consequences on the overall helical parameters, in that a deviation from classical B-DNA is observed. This is easily recognized by looking along the helical axis, realizing that the base-pair centers are no longer crossed by the helical axis but are set off. Extrapolating to isopentyl-containing oligonucleotides, this could explain the structural differences, observed by CD spectroscopy, of duplexes **2.4** and **5.2S · 5.2A** relative to their unmodified duplexes and may reflect, at least in part, the destabilizing effect of the alkyl modification.

As representatives of the structural motif **III**, we modeled the duplexes **6.1S · 6.1A** and **6.2S · 6.2A** (*Fig. 10*). In this case, we also attempted to include structural differences that might occur as a function of the nature of the side chain (butyl *vs.* isopentyl). As can be seen, the motif in general corrects for the eclipsed alkyl modifications across the minor groove as compared to motif **II**. The butyl-modified duplex (*Fig. 10*, *a* and *c*) shows no explicit alkyl zipper. The butyl-chains are too far

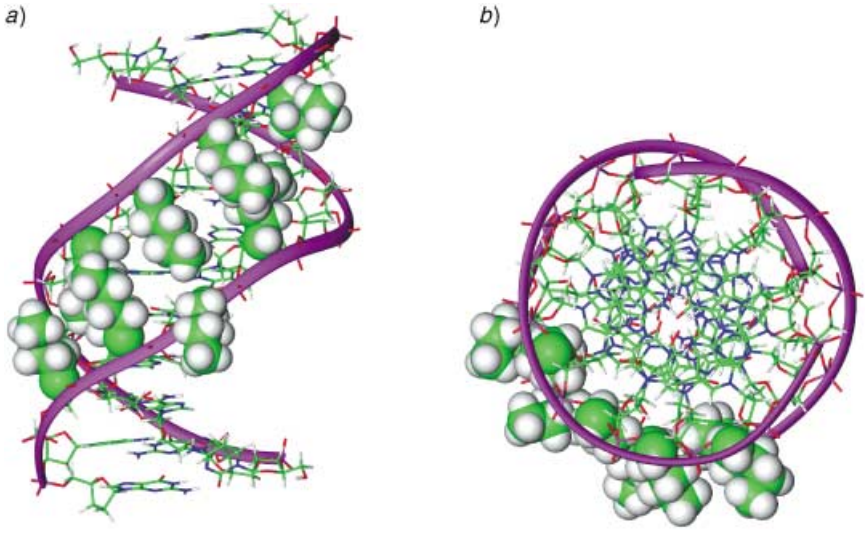

Fig. 9. *Molecular-dynamics simulation* (200 ps trajectory, amber force field) *of duplex* **2.4**: *averaged structure of the last 100 ps viewed* a) *perpendicular to and* b) *along the helical axis*

apart from each other. Introduction of branched chain alkyl residues, as the isopentyl group, corrects for this in part (*Fig. 10*,*b* and *d*). This duplex not only shows groups of alkyl residues that are tightly aligned to each other, it also shows less distorsion of the overall helical parameters of B-DNA as can be seen from the view along the helical axis.

3. Conclusions. – In the present study, we have shown that 5′-butyl or 5′-isopentyl modifications in oligonucleotides lead to a reduction in thermodynamic stability irrespective of their sequential arrangement. By UV-melting-curve analysis, ITC, CD spectroscopy, and molecular modeling, we found, however, that within the proposed structural model **III**, accommodation of alkyl residues without extended distorsion of the helical parameters of B-DNA is possible. Thus, according to modelling of the structure of the duplex **6.2S** · **6.2A**, the initially postulated zipper motif seems possible but might require larger or more highly branched alkyl side chains. The most densely packed motif **II** seems to suffer from an ecliptic arrangement of opposite alkyl groups which might account for the systematic negative contribution to stability due to steric reasons. If there exists alkyl-zipper formation in the class-**III** oligonucleotides, there is no contribution to duplex stability, as favorable hydrophobic interactions might be overcompensated by loss of structured H_2O in the minor groove. Furthermore, the thermodynamic analysis points to differential stabilization of the single-strand structures as the main factors dominating duplex stability.

The authors wish to thank the *Swiss National Science Foundation* for continuous support of our work in the field of oligonucleotide chemistry.

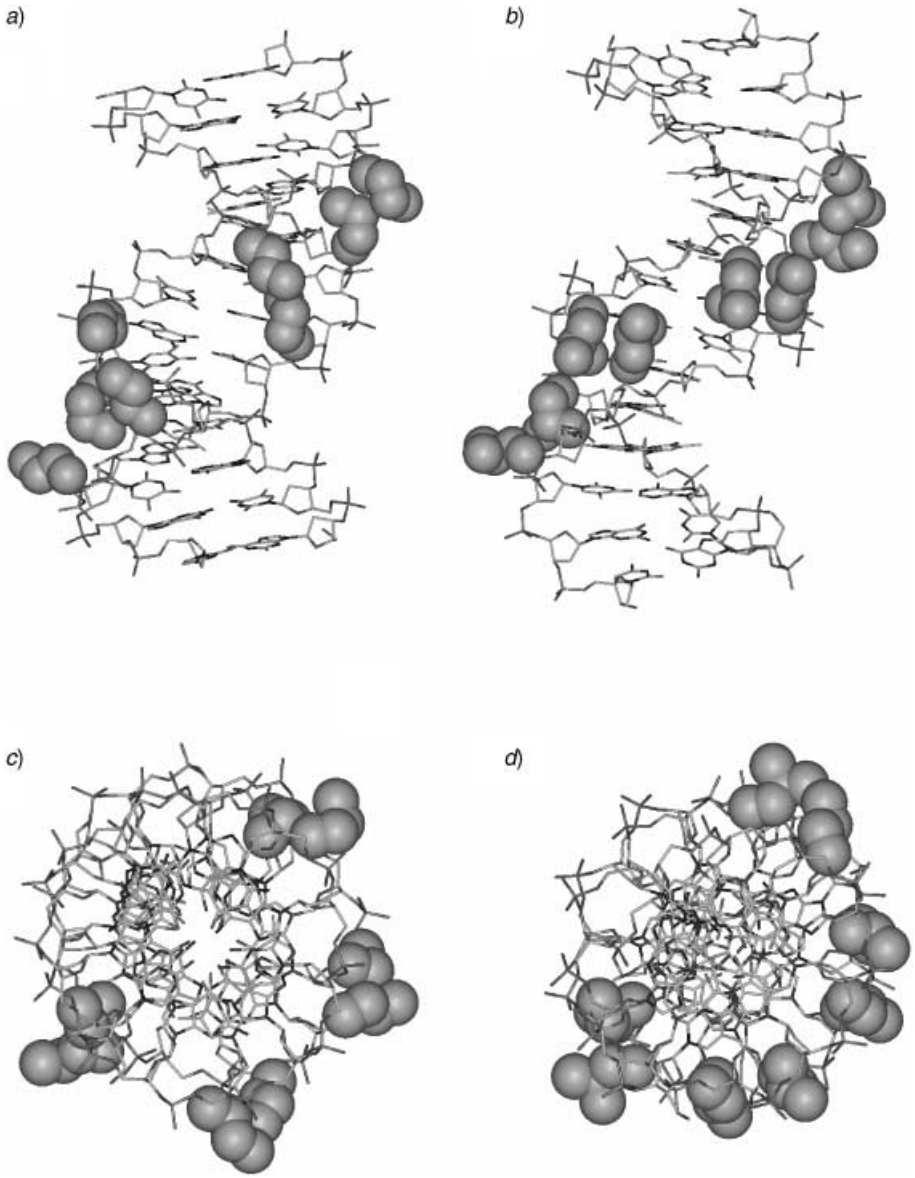

Fig. 10. *Averaged structures of the last 50 ps of a molecular-dynamics simulation* (200 ps trajectory, amber force field) *of* a) c) *duplexes* **6.1S** · **6.1A** *and* b) d) *duplex* **6.2S** · **6.2A**. *Views perpendicular* a) b) *and parallel* c) d) *to the helix axes.* The butyl and isopentyl side chains are highlighted in grey as CPK models.

Experimental Part

Oligodeoxynucleotide Synthesis. Oligodeoxynucleotides were synthesized on a *Pharmacia Gene Assembler Special* connected to a *Compaq-ProLinea-3/25-zs* personal computer. Nonnatural phosphoramidites (0.1M in MecN) and 1*H*-tetrazole (0.5M in MeCN) were equal in concentration to those used for the synthesis of natural oligonucleotides. For the introduction of the 5′-alkylnucleosides, the coupling time was raised to 10 min, and for natural nucleosides following a modified one, it was raised to 5 min. Coupling efficiencies as monitored by the on-line trityl assay were generally higher than 98% for natural nucleosides and higher than 96% for the 5′-alkylnucleosides. The last step in every synthesis was the removal of the 5′-protecting group (trityl-off mode). After the synthesis, the solid support was suspended in conc. NH_3 soln. and left for 18 h at 55° to effect deprotection. Filtration and evaporation yielded the crude oligodeoxynucleotides that were subsequently purified by HPLC (*Table 8*). UV-Spectroscopically determined yields after chromatographic purification were in the range of 17–59% (*Table 8*). All oligonucleotides prepared were subjected to MALDI-TOF-MS analysis (*Table 9*).

UV Melting Curves. A *Varian-Cary-3E*-UV/VIS spectrophotometer equipped with a temp.-controller unit and connected to a *Compaq-ProLinea-3/25-zs* personal computer was used. A temp. gradient of 0.5°/min was applied, and data points were collected in intervals of *ca.* 0.5°. At temp. $< 20°$, the cell compartment was flushed with N_2 to prevent condensation of H_2O on the UV cells. The transition temperature T_m was defined as the maximum of the first derivative of the UV-melting curve.

CD Spectra. A *Jasco-715* spectropolarimeter with a 150W Xe high-pressure lamp was connected to a personal computer. Thermostatting of the cell holder was effected by a *Jasco PDF-350S-Peltier* element, coupled with a *Colora K5* ultrathermostat. The temp. was determined directly in the sample soln.

Isothermal Titration Calorimetry (ITC). An *Omega* isothermal titration calorimeter (*MicroCal Inc.,* Northampton, MA, USA) was connected to a *Grant LTD-6* cooling device, interfaced to a personal computer, and controlled by the Origin ITC V 2.90 software. All measurements were performed in 150 mM NaCl, 10 mM NaH_2PO_4, pH 7, at $30.5 \pm 0.5°$. Sample-cell volume, 1.3267 ml. One oligonucleotide strand (11.1–12.3 μM soln. in buffer) was placed in the cell, and the complementary oligonucleotide strand (101.9–132.8 μM soln. in buffer) was placed in a 250-μl precision syringe, the needle of which was paddle-shaped and rotated at 400 rpm. The syringe plunger was mechanically coupled to a computer-controlled stepping motor. In all experiments, 24 aliquots of 10–12 μl, amounting to a total of 2.0 equiv. of titrant, were added at 5-min intervals. The integrated heats of interaction were fitted by the Origin for ITC (*MicroCal*) software by means of the single-interaction-site fitting function. All experiments were performed in triplicate, and mean values and standard deviations were determined.

Molecular Modelling. All calculations were performed with Insight II/Discover (vers. 97) from *Molecular Simulation Inc.* The modified base pairs were constructed with the templates available from *Biopolymer*. Oligonucleotide duplexes were generated with the parameters for B-DNA. The structures were calculated with the Amber forcefield as implemented in Discover. Instead of explicit H_2O molecules, a distance-dependent dielectricity constant of *4r* was used. Nonbonding interactions were scaled by a factor 0.5. The structures were minimized to a gradient of 0.05 kcal/(mole · Å) first by using a 'steepest-descent' gradient, then with a 'conjugate-gradient' algorithm. The minimized structures were warmed from 0 to 300 K within 20 ps and were held at this temp. for 200 ps. Structures were recorded every 0.5 ps. The structures of the last 50 ps of the dynamics simulation were averaged and the resulting geometries fully minimized.

Table 8. *Synthesis and HPLC Data of Oligodeoxynucleotides*

	Sequence	Scale [μmol]	Purification[a])	t_R [min]	*OD* (260 nm)	Yield [%]
1.0	d(GCGCTTTTAAAAGCGC)	1.30	AE 40–70% B^1 in 30 min	23.8	61.5	41
			RP 10–30% B in 25 min	14.0		
1.4	d(GCGCT$_B$T$_B$T$_B$T$_B$AAAAGCGC)	1.25	AE 44–59% B^1 in 25 min, then 100% B^1 in 15 min	*ca.* 30	24.9	17
			RP 10–30% B in 25 min	24.2		
2.0	d(GCGCAAAATTTTGCGC)	1.32	AE 40–70% B^1 in 30 min	27.7	57.0	38
			RP 10–30% B in 25 min, then 100% B in 8 min	22.8		
2.4	d(GCGCAAAAT$_B$T$_B$T$_B$T$_B$GCGC)	1.29	AE 40–51% B^2 in 30 min	18.0	43.1	29
			RP 10–35% B in 25 min, then 100% B in 8 min	25.2		
3.0	d(GATATATATATATC)	1.34	AE 33–40% B^2 in 20 min	17.8	88.0	59
			RP 10–30% B in 25 min, then 100% B in 8 min	15.2		
3.1	d(GATAT$_B$AT$_B$AT$_B$AT$_B$AT$_B$C)	1.34	AE 38–43% B^2 in 20 min, then 43–100% B^2 in 5 min	20.6	75.6	51
			RP 10–30% B in 25 min, then 100% B in 8 min	19.8		
5.0S	d(TACAGGACCTCAGT)	1.30	AE 28–38% B^2) in 20 min, then 38–100% B^2 in 5 min	22.8	43.8	30
			RP 10–30% B in 25 min	12.2		
5.1S	d(TACAGGAC$_B$C$_B$T$_B$C$_B$AGT)	1.30	AE 35–44% B^2 in 20 min, then 44–100% B^2 in 5 min	21.2	45.0	31
			RP 10–50% B in 25 min	19.8		
5.2S	d(TACAGGAC$_i$PC$_i$PT$_i$PC$_i$PAGT)	1.44	AE 38–44% B^2 in 22 min, then 44–100% B^2 in 5 min	23.1	44.4	28
			RP 10–50% B in 25 min	24.0		
5.0A	d(ACTGAGGTCCTGTA)	1.30	AE 30–38% B^2 in 20 min, then 38–100% B^2 in 5 min	23.0	41.1	28
			RP 10–30% B in 25 min	12.7		
5.1A	d(ACTGAGGT$_B$C$_B$C$_B$T$_B$GTA)	1.30	AE 38–44% B^2 in 20 min, then 44–100% B^2 in 5 min	21.1	37.1	25
			RP 10–50% B in 25 min	19.2		
5.2A	d(ACTGAGGT$_{iP}$C$_{iP}$C$_{iP}$T$_{iP}$GTA)	1.42	AE 38–44% B^2 in 22 min, then 44–100% B^2 in 5 min	23.4	39.2	24
			RP 10–55% B in 25 min	20.7		
6.0S	d(GCATACGTACACCG)	1.30	AE 30–38% B^2 in 20 min, then 38–100% B^2 in 5 min	27.1	77.1	52
			RP 10–30% B in 25 min	12.0		
6.1S	d(GCATAC$_B$GT$_B$AC$_B$AC$_B$CG)	1.30	AE 38–44% B^2 in 20 min, then 44–100% B^2 in 5 min	27.2	56.8	38
			RP 10–50% B in 25 min	16.8		
6.2S	d(GCATAC$_{iP}$GT$_{iP}$AC$_{iP}$AC$_{iP}$CG)	1.33	AE 42–50% B^2 in 20 min, then 50–100% B^2 in 5 min	26.8	31.9	21
			RP 10–55% B in 25 min	18.3		
6.0A	5′-d(CGGTGTACGTATGC)	1.30	AE 30–40% B^2 in 20 min, then 40–100% B^2 in 5 min	22.8	47.5	32
			RP 10–30% B in 25 min	10.8		
6.1A	d(CGGTGT$_B$AC$_B$GT$_B$AT$_B$GC)	1.30	AE 38–45% B^2 in 20 min, then 45–100% B^2 in 5 min	22.4	47.3	32
			RP 10–50% B in 25 min	16.6		
6.2A	d(CGGTGT$_{iP}$AC$_{iP}$GT$_{iP}$AT$_{iP}$GC)	1.41	AE 42–50% B^2 in 20 min then 50–100% B^2 in 5 min	23.2	54.4	33
			RP 10–55% B in 25 min	17.6		

[a]) AE = Anion-exchange chromatography: *Nucleogen DEAE 60-7*, 125 × 4 mm, with *Nucleogen-Guard* column 30 × 4 mm (*Machery&Nagel*); solvent A^1 = 20 mM KH_2PO_4, pH 6, in H_2O/MeCN 8 : 2, and solvent B^1 = 20 mM KH_2PO_4, 1M KCl in H_2O/MeCN 8 : 2; solvent A^2 = 20 mM NaH_2PO_4, pH 6, in H_2O/MeCN 7 : 3; and solvent B^2 = 20 mM NaH_2PO_4, 1M NaCl in H_2O/MeCN 7 : 3. RP = reversed-phase chromatography: *Aquapore RP-300*, 220 × 6 mm (7 μm) with *RP-C8 Newguard* (7 μm) (*Brownlee Labs*); solvent A = 0.10M (Et_3NH)OAc in H_2O and solvent B = 0.10M (Et_3NH)OAc in H_2O/MeCN 1 : 4. All gradients were started at the indicated amount of solvent B and at the end washed for 8 min with 100% B and reconditioned for 8 min with the starting mixture. All chromatographic purifications were done at a flow rate of 1 ml/min. and at 60°, and compounds were detected by UV at 260 nm.

Table 9. *Molecular Masses of Oligonucleotides Measured by MALDI-TOF MS*

	Oligonucleotide	Calc. for $[M-H]^-$	Found for $[M-H]^-$
1.0	d(GCGCTTTTAAAAGCGC)	4881.2	4879.1
1.4	d(GCGC$T_BT_BT_BT_B$AAAAGCGC)	5105.7	5103.8
2.0	d(GCGCAAAATTTTGCGC)	4881.2	4879.1
2.4	d(GCGCAAAA$T_BT_BT_BT_B$GCGC)	5105.7	5105.8
3.0	d(GATATATATATATC)	4260.9	4258.0
3.1	d(GAT$AT_BAT_BAT_BAT_B$C)	4539.4	4541.6
5.0S	d(TACAGGACCTCAGT)	4303.0	4306.9
5.1S	d(TACAGGA$C_BC_BT_BC_B$AGT)	4527.4	4529.0
5.2S	d(TACAGGA$C_{iP}C_{iP}T_{iP}C_{iP}$AGT)	4583.5	4586.0
5.0A	d(ACTGAGGTCCTGTA)	4319.9	4322.1
5.1A	d(ACTGAGGT$C_BC_BC_BT_B$GTA)	4544.37	4545.2
5.2A	d(ACTGAGGT$C_{iP}C_{iP}C_{iP}T_{iP}$GTA)	4600.5	4600.2
6.0S	d(GCATACGTACACCG)-	4302.0	4300.8
6.1S	d(GCATAC$_B$GTAC$_B$AC$_B$CG)	4526.4	4526.4
6.2S	d(GCATAC$_{iP}$GT$_{iP}$AC$_{iP}$AC$_{iP}$CG)	4582.5	4582.9
6.0A	d(CGGTGTACGTATGC)-3′	4321.9	4322.1
6.1A	d(CGGTGT$_B$AC$_B$GT$_B$AT$_B$GC)	4546.3	4542.1
6.2A	d(CGGTGT$_{iP}$AC$_{iP}$GT$_{iP}$AT$_{iP}$GC)	4602.45	4601.8

REFERENCES

[1] P. Herdewijn, *Liebigs Ann. Chem.* **1996**, 1337.
[2] M. Meldgaard, J. Wengel, *J. Chem. Soc., Perkin Trans. I* **2000**, 3539.
[3] C. J. Leumann, *Bioorg. Med. Chem.* **2002**, *10*, 841.
[4] V. A. Buckin, B. I. Kankiya, N. V. Bulichov, A. V. Lebedev, I. Y. Gukovsky, V. P. Chuprina, A. P. Sarvazyan, A. R. Williams, *Nature (London)* **1989**, *340*, 321.
[5] N. J. Tao, S. M. Lindsay, A. Rupprecht, *Biopolymers* **1989**, *28*, 1019.
[6] T. Umehara, S. Kuwabara, S. Mashimo, S. Yagihara, *Biopolymers* **1990**, *30*, 649.
[7] A. Ben Naim, K. L. Ting, R. L. Jernigan, *Biopolymers* **1990**, *29*, 901.
[8] M. Egli, V. Tereshko, M. Teplova, G. Minasov, A. Joachimiak, R. Sanishvili, C. M. Weeks, R. Miller, M. A. Maier, H. An, C. P. Dan, M. Manoharan, *Biopolymers* **1998**, *48*, 234.
[9] J. N. Glover, S. C. Harrison, *Nature (London)* **1995**, *373*, 257.
[10] G. Wang, P. J. Middleton, *Tetrahedron Lett.* **1996**, *37*, 2739.
[11] G. Wang, P. J. Middleton, Y.-Z. An, *Tetrahedron Lett.* **1997**, *38*, 2393.
[12] G. Wang, P. J. Middleton, C. Lin, Z. Pietrzkowski, *Bioorg. Med. Chem. Lett.* **1999**, *9*, 885.
[13] H. U. Trafelet, E. Stulz, C. Leumann, *Helv. Chim. Acta* **2001**, *84*, 87.
[14] M. Tarköy, M. Bolli, C. Leumann, *Helv. Chim. Acta* **1994**, *77*, 716.
[15] G. Vesnaver, K. J. Breslauer, *Proc. Natl. Acad. Sci. U.S.A.* **1991**, *88*, 3569.

Received August 16, 2003